

Biogeosciences Discussions is the access reviewed discussion forum of *Biogeosciences*

Towards a more harmonized processing of eddy covariance CO₂ fluxes: algorithms and uncertainty estimation

D. Papale¹, M. Reichstein², E. Canfora¹, M. Aubinet³, C. Bernhofer⁴,
B. Longdoz⁵, W. Kutsch², S. Rambal⁶, R. Valentini¹, T. Vesala⁷, and D. Yakir⁸

¹Department of Forest Science and Environment, University of Tuscia, 01100 Viterbo, Italy

²Max-Planck Institut fur Biogeochemie, P.O. Box 100164, 07701 Jena, Germany

³Unité de Physique des Biosystèmes, Faculté Universitaire des Sciences Agronomiques de Gembloux, 5030 Gembloux, Belgium

⁴Department of Meteorology, Institute of Hydrology and-Meteorology, Technische Universität Dresden, 01062 Dresden, Germany

⁵Ecologie et Ecophysiologie Forestières, Centre de Nancy, 54280 Champenoux, France

⁶Dream CEFE-CNRS, 1919 route de Mende, 34293 Montpellier, France

⁷Department of Physical Sciences, University of Helsinki, P.O. Box 64, 00014, Finland

⁸Department of Environmental Sciences and Energy Research, Weizmann Institute of Science, P.O. Box 26, 76100 Rehovot, Israel

Received: 7 June 2006 – Accepted: 29 June 2006 – Published: 13 July 2006

Correspondence to: D. Papale (darpap@unitus.it)

**Algorithms and
uncertainty
processing eddy
covariance data**

D. Papale et al.

Title Page

Abstract

Introduction

Conclusions

References

Tables

Figures

⏪

⏩

◀

▶

Back

Close

Full Screen / Esc

Printer-friendly Version

Interactive Discussion

Abstract

Eddy covariance technique to measure CO₂, water and energy fluxes between biosphere and atmosphere is widely spread and used in various regional networks. Currently more than 250 eddy covariance sites are active around the world measuring carbon exchange at high temporal resolution for different biomes and climatic conditions. These data are usually acquired using the same method but they need a set of corrections that are often differently applied to each site and in a subjective way. In this paper a new standardized set of corrections are proposed and the uncertainties introduced by these corrections are assessed for 8 different forest sites in Europe with a total of 12 yearly datasets. The uncertainties introduced on the two components GPP (Gross Primary Production) and TER (Terrestrial Ecosystem Respiration) are also discussed and a quantitative analysis presented. The results show that a standardized data processing is needed for an effective comparison across biomes and for underpinning inter-annual variability. The methodology presented in this paper has also been integrated in the European database of the eddy covariance measurements.

1 Introduction

The eddy covariance technique provides unique measurements of CO₂, water and energy fluxes between the biosphere and the atmosphere at the ecosystem scale. Currently, more than 250 eddy covariance towers are acquiring data around the world (Baldocchi et al., 2001), covering different climate conditions, land cover and management classes, some of them running continuously for more than 10 years. The eddy covariance technique is based on high frequency (10–20 Hz) measurements of wind speed and direction as well as CO₂ and H₂O concentrations at a point over the canopy using a three-axis sonic anemometer and a fast response infrared gas analyzer (Aubinet et al., 2000, 2003a). Assuming perfect turbulent mixing these measurements are typically integrated over periods of half an hour (Goulden et al., 1996) building the basis

BGD

3, 961–992, 2006

Algorithms and uncertainty processing eddy covariance data

D. Papale et al.

Title Page

Abstract

Introduction

Conclusions

References

Tables

Figures

⏪

⏩

◀

▶

Back

Close

Full Screen / Esc

Printer-friendly Version

Interactive Discussion

to calculate carbon and water balances from daily to annual time scales.

There are different sources of uncertainties in the eddy covariance measurements that sometimes difficult to assess. Random measurement errors due to the technique have been assessed by Hollinger and Richardson (2005), comparing the measurements from two towers with the same flux source area (“footprint”) and by Richardson et al. (2006), comparing pair of measurements made on two successive days from the same tower under equivalent environmental conditions. Varying footprints can be a source of errors and uncertainties that can affect the data quality, particularly if the ecosystem is inhomogeneous (Göckede et al., 2004). In addition, several errors due to instrumentation limits may appear (acquisition frequency, sensor separation, fluctuation attenuation in closed systems, etc. . .). Most of these problems can be solved by applying correction procedures accordingly. However, it was shown by different authors (Aubinet et al., 2000; Goulden et al., 1996; Gu et al., 2005), independently of the preceding problems, eddy flux measurements can underestimate the net ecosystem exchange during periods with low turbulence and air mixing. This underestimation acts as a selective systematic error: it only occurs during the night when CO₂ is produced by the ecosystem. As a consequence, the ecosystem respiration is underestimated and the carbon sequestration overestimated (Moncrieff et al., 1996).

Massman and Lee (2002) listed the possible causes of the night flux error. There is now a large consensus to recognise that the most probable cause of error is the presence of small scale movements associated with drainage flows or land breezes that take place in low turbulence conditions and create a decoupling between the soil surface and the canopy top. In these conditions, advection becomes an important term in the flux balance and can no more be neglected. It was recently suggested (Finnigan et al., 2006) that, contrary to what was thought before, advection probably affects most of the sites, including flat and homogeneous ones. Direct advection flux measurements are difficult to measure as they require several measurement towers at the same site. Attempts were made notably by Aubinet et al. (2003b), Feigenwinter et al. (2004), Staebler and Fitzjarrald (2004) and Marcolla et al. (2005). They found

BGD

3, 961–992, 2006

Algorithms and uncertainty processing eddy covariance data

D. Papale et al.

Title Page

Abstract

Introduction

Conclusions

References

Tables

Figures

⏪

⏩

◀

▶

Back

Close

Full Screen / Esc

Printer-friendly Version

Interactive Discussion

that advection fluxes were usually significant during calm nights. However, in most cases, the measurement uncertainty was too large to allow their precise estimation. In addition, such direct measurements require a too complicated set up to allow routine measurements at each site.

5 In practice, the night flux problem is by-passed by discarding the data corresponding to low mixed periods and replacing them by an assessment based either on the parameterisation of the night flux response to the climate or on look up tables (Falge et al., 2001; Papale and Valentini, 2003; Reichstein et al., 2005). The friction velocity is currently used as a criterion to discriminate low and well mixed periods. This approach
10 is generally known as the “ u_* correction”.

Although being the best and most widely method currently used to circumvent the problem, the u_* correction is affected by several drawbacks and must be applied with care.

15 First, an implicit application of the correction could lead to even bigger errors: indeed, during calm night conditions, the CO_2 can be either removed by advection or stored in the canopy air. In the first case, the application of a u_* correction is fully justified. However, in the second case, the CO_2 stored in the canopy air would be removed by the turbulence as soon as it restarts. It would be captured at this moment by the eddy covariance system. If a u_* correction had been applied during the storage period, this
20 flux would thus have been counted twice. One way to avoid this problem is to first correct the data for storage and then apply the u_* selection. However, this requires reliable CO_2 storage measurements which are not always available at all sites.

The best way to compute storage flux is to deduce it from CO_2 concentration profiles made in the canopy. However, at many sites, a discrete estimation based only on the concentration at the tower top is used. It is likely that, in tall forests sites, such an
25 estimation is insufficient as it does not take the large concentration increase in the lower air layers into account. It is therefore important to understand the potential errors introduced using the discrete approach instead of the profile system.

Another problem with the u_* correction is that it depends on the operator’s subjectiv-

**Algorithms and
uncertainty
processing eddy
covariance data**D. Papale et al.

Title Page

Abstract

Introduction

Conclusions

References

Tables

Figures

⏪

⏩

◀

▶

Back

Close

Full Screen / Esc

Printer-friendly Version

Interactive Discussion

ity. Indeed, the u_* threshold used to discriminate well and poorly mixed data is generally chosen by visual inspection. Different alternative heuristic methods were proposed to automatically determine the appropriate u_* threshold value (Gu et al., 2005; Reichstein et al., 2003, 2005).

5 Finally, the hypotheses underlying the u_* correction are still debatable: firstly it is based on the assumption that flux in calm conditions can be inferred from measurements made in windy conditions, which is not proved. Secondly, it supposes that measurements made during turbulent periods are free of errors which is questioned by recent experiment results (Kolle, private communication, Cook et al., 2004; Wohlfahrt et al., 2005).

10 In this context it is important to have a set of tools to process all the datasets available with a standardized method with the aim to improve their quality, particularly if the data are used for interannual analysis or site intercomparisons, and where raw data are not available. In particular there is a high heterogeneity in terms of quality and methods used in data processing. Many improvements in the Eddy measurements treatments were presented and applied over the last 10 years, often detailed information about the data processing methods were not available and important variables like the CO_2 storage under the canopy were not measured. For this reason it is very important to find a standardized method to reprocess also the old data and obtain a standardized dataset.

20 It is also crucial to assess the effect of these corrections on data and the errors and uncertainties introduced. The sequence of analyses presented in this paper is based solely on the data to find the half-hourly data affected by common problems like spikes or low turbulence. Methodological uncertainties introduced by the different quality control procedures (e.g. u_* threshold selection) are systematically assessed at daily to annual time scales. Moreover, we also want to scientifically document the data processing applied in the CarboeuropelP Ecosystem database (<http://gaia.agraria.unitus.it/database>) that now comprises more than 100 sites and a total of more that 250 site-years.

**Algorithms and
uncertainty
processing eddy
covariance data**D. Papale et al.

Title Page

Abstract

Introduction

Conclusions

References

Tables

Figures

⏪

⏩

◀

▶

Back

Close

Full Screen / Esc

Printer-friendly Version

Interactive Discussion

2 Materials and methods

2.1 Site and processing overview

For these analyses, 12 annual datasets of CO₂ exchange have been used from eight European eddy covariance sites (Table 1). The data were first storage corrected, then a spike detection technique was applied and, after that, filtered for low turbulence conditions (low u_*). After these checks the yearly datasets were gap filled and the two components Gross Primary Production (GPP) and Terrestrial Ecosystem Respiration (TER) were estimated.

2.2 The spike detection method

Eddy covariance measurements are often affected by spikes, due to different reasons both bio-physical (changes in the footprint or fast changes in turbulence conditions) and instrumental (e.g. water drops on sonic anemometer or on open path IRGA). The spikes affecting the single instantaneous measurement (high frequency spikes) are removed before the half-hourly average is calculated. Spikes could however remain in the half hourly values and an outlier detection technique was applied to find these occasional spikes in the half-hourly flux data. These spikes commonly do not affect directly the annual sums but can affect the quality of the gapfilled datasets. The algorithm used to detect the spikes is based on the position of each half hourly value with respect to the values just before and after and it is applied to blocks of 13 days and separately for daytime and nighttime data. The outliers detection was based on the double-differenced time series, using the median of absolute deviation about the median (MAD) that is a robust outlier estimator (Sachs, 1996).

For each NEE_i half hourly data the d value is calculated as:

$$d_i = (NEE_i - NEE_{i-1}) - (NEE_{i+1} - NEE_i) \quad (1)$$

BGD

3, 961–992, 2006

**Algorithms and
uncertainty
processing eddy
covariance data**

D. Papale et al.

Title Page

Abstract

Introduction

Conclusions

References

Tables

Figures

⏪

⏩

◀

▶

Back

Close

Full Screen / Esc

Printer-friendly Version

Interactive Discussion

and the value is flagged as spike if:

$$Md + \left(\frac{z \times MAD}{0.6745} \right) > d_i > Md - \left(\frac{z \times MAD}{0.6745} \right) \quad (2)$$

where Md is the median of the differences, MAD is defined as

$$MAD = \text{median} (|d_i - Md|) \quad (3)$$

5 and z is a threshold value.

Different z values were used to assess the effect on the data and the sensibility of the method. In particular in this study we used three z values: 4, that is conventionally used and – to be more conservative – 5.5 and 7.

2.3 The u_* threshold selection and uncertainty

10 The u_* -threshold was specifically derived for each site using a 99% threshold criterion on night-time data as described by Reichstein et al. (2005): night-time data was selected according to a global radiation threshold of 20 Wm^{-2} , cross-checked against sunrise and sunset data derived from the local time and standard sun-geometrical routines. For the u_* -filtering, the data set is split into six temperature classes of equal
15 sample size (according to quantiles) and for each temperature class, the set is split into 20 equally sized u_* -classes. The threshold is defined as the u_* -class where the night-time flux reaches more than 99% of the average flux at the higher u_* -classes. The threshold is only accepted if for the temperature class, temperature and u_* are not or only weakly correlated ($|r| < 0.4$) The final threshold is defined as the median of
20 the thresholds of the (up to) six temperature classes. This procedure is applied to the subsets of four 3-month periods (January–March, April–June, July–September and October–December) to account for seasonal variation of vegetation structure.

The u_* -threshold is reported for each period, but the whole data set is filtered according to the highest threshold found (conservative approach). In cases where no
25 u_* -threshold could be found with this approach, it is set to the 90% percentile of the

Title Page

Abstract

Introduction

Conclusions

References

Tables

Figures

⏪

⏩

◀

▶

Back

Close

Full Screen / Esc

Printer-friendly Version

Interactive Discussion

data (i.e. a minimum 10% of the data are retained). A minimum threshold is set to 0.1 ms^{-1} for forest canopies and 0.01 ms^{-1} for short vegetation sites that commonly have lower u_* values. To be more conservative, in addition to the data acquired when u_* was below the threshold, the first half hour measured with good turbulence conditions after a period with low turbulence is also removed.

This procedure is repeated 100 times within a bootstrapping technique to assess the uncertainty of the u_* threshold detection, where the whole annual dataset is bootstrapped (Efron and Tibshirani, 1993). The 5% and 95% percentiles of the 100 bootstrapped threshold estimates are taken as confidence interval boundaries (Fig. 1).

2.4 Gap filling and partitioning used

To compare the effect of the different checks and filters applied at different time resolution (from daily to annual), all the datasets had to be filled. We used as gap-filling techniques the method described in Reichstein et al. (2005) that exploits both the covariation of fluxes with meteorological variables and the temporal autocorrelation of fluxes. The potential effect of different gap-filling methods on annual sums is out of the scope of this paper, but it is systematically addressed in an ongoing work by Moffat et al. 2006¹) and seems to be generally small for the methods investigated (Papale et al., 2005).

The partitioning between Gross Primary Production and Terrestrial Ecosystem Respiration has been done according with the method proposed in Reichstein et al. (2005).

¹Moffat, A., Papale, D., Reichstein, M., et al.: Gap filling methods intercomparison, in preparation, 2006.

Title Page

Abstract

Introduction

Conclusions

References

Tables

Figures

⏪

⏩

◀

▶

Back

Close

Full Screen / Esc

Printer-friendly Version

Interactive Discussion

3 Results and discussion

3.1 Variability and uncertainty of u_* threshold values

For the 12 site/years used in this analysis, the 3 different u_* thresholds obtained after storage correction and spike detection are in a range that varies between 0.1 and 0.7 ms^{-1} , as reported in Fig. 2. Noteworthy, the u_* threshold can be completely different for different sites, from very low values and low uncertainty as in FR01 to high values and uncertainty as in DE03. This variability in the u_* threshold between sites is possibly due to characteristics like vegetation and measurement heights, land-use and topography. The value and the amplitude of the uncertainty in the threshold selected is however not always directly related to the uncertainty introduced in the data and this will be shown later in the paper.

3.2 Effect of storage and u_* correction

According to the eddy covariance data processing method, the CO_2 fluxes are corrected by storage fluxes and after that filtered by u_* to remove measurements acquired during low turbulence conditions. These two corrections have to be done in the order described above to avoid the double counting effect, i.e. that (turbulent+storage) fluxes are removed during night with low u_* (and so the potentially high storage flux ignored) while during the following morning the depletion of the storage is accounted for (Aubinet et al., 2002). Figure 3 shown the annual sums obtained for the different sites/years by using different treatments : the recommended one (first storage, then u_*), u_* correction only, storage correction only, and no correction. The little differences between data without corrections and data only storage corrected, that theoretically should be exactly the same for the annual sum, are due to the different number of gaps (e.g. if storage flux is missing, but not turbulent flux). It is possible to see that the differences between the four annual sums presented for each site and year vary a lot from site to site. For example for FR01 the differences are in the order of 30–40 $\text{gC m}^{-2} \text{yr}^{-1}$ (be-

BGD

3, 961–992, 2006

**Algorithms and
uncertainty
processing eddy
covariance data**

D. Papale et al.

Title Page

Abstract

Introduction

Conclusions

References

Tables

Figures

⏪

⏩

◀

▶

Back

Close

Full Screen / Esc

Printer-friendly Version

Interactive Discussion

tween 5 and 10%) while for IT03 the differences are very strong and lead to changes the site from sink to source. Another interesting point is that the double counting problem (differences between right correction and only u_*) is evident only for part of the sites (BE01, DE02, FR04, IL01 and IT03) while for other sites is not clear (in FI01 and FR01 the trend changes from one year to the other) or in the opposite direction as expected (DE03).

3.3 Effect of the filtering techniques used

The amount of data removed by the filtering algorithms was found variable as depicted in Table 2. The “Missing” column indicates the percentage of missing NEE values (not measured or affected by evident measurement problems like pump or gas analyzer broken); columns labelled as “Spike” are relative to the percentages of additionally removed data, due to spike detection, using the three different thresholds. An example of the data detected as spikes is also shown in Fig. 4. The three “Ustar” columns of Table 2 show the percentages of additionally removed data because acquired under stable conditions (with low u_*) according with the three thresholds used. The last column lists the percentages of data removed using a “mean” configuration with spike threshold 5.5 and 50% u_* threshold. It is evident that the largest percentages of data is removed by the u_* filtering, while the spike removal keeps largest part of the data untouched. Up to more than 50% of the night-time data are subject to this u_* -based filter, while daytime data are less affected by turbulence problems, except for DE03 where in 2002 up to 50% of daytime data were filtered with the highest u_* threshold.

All the corrections and checks described above have an effect at different time scales, from the average daily trend to the annual sums. Figure 5 shows the monthly mean diurnal NEE trends of the day for three site/years obtained using three different storage correction: with the storage term assessed using a CO_2 concentration profile in the canopy (NEE_pr), assessed using the discrete approach using only the CO_2 concentration measured on the top of the tower (NEE_sp) and without any storage correction (Fc). Looking at the residuals, we note that without any storage correction a systematic

Title Page

Abstract

Introduction

Conclusions

References

Tables

Figures

⏪

⏩

◀

▶

Back

Close

Full Screen / Esc

Printer-friendly Version

Interactive Discussion

error is introduced during both day and night time. The two errors go in the opposite direction with underestimation of night-time respiration and overestimation of daytime carbon uptake. It is also clear that the effect of the storage correction is different in the three sites, with minor effect for FI01 (Fig. 5c). Analyzing the differences between the two storages it appears that the differences are lower in respect to the comparison between storage and no storage correction at all and also the pattern is different and less systematic.

Figure 6 shows the effect of the different thresholds z in the spike removing algorithm. The average daily trend has been calculated after filtering the data according with the $3z$ values of 4, 5.5 and 7 and also without performing the spike detection at all. It is important to remark that the presence of spikes is related to different aspects and in particular to the site characteristics but also to the data screening operated by the PI. It is possible to see that the spike removing affects the mean diurnal trend less than the storage correction. In addition, there is not a clear trend also if it seems that the major part of spikes for DE03 has been detected as “respiration” spikes.

The analysis of the average daily trends does not give a clear quantitative information about the effect on the daily to annual budget. We characterise the intrinsic uncertainties of the correction methods by the difference between the maximum flux and minimum flux obtained depending on the method for each day, week or month. These uncertainties are presented in Fig. 7 as box-plots, where for example the median range of the different methods for daily fluxes was $0.4 \text{ gC m}^{-2} \text{ day}^{-1}$, considered as the median uncertainty of the corrections applied. As expected, the uncertainty is bigger in the daily sums compared to 8-daily and monthly aggregations. The u_* threshold selection is the most important source of uncertainty while storage, and in particular spike detection, have a smaller effect on the sums.

To understand the correction effects on annual sums an ANOVA has been performed using the data coming from the sites where the storage is measured also using the profile system. The summary of the results are shown in Fig. 8. The main source of uncertainty is confirmed to be u_* that is the main factor for three sites and in the

[Title Page](#)[Abstract](#)[Introduction](#)[Conclusions](#)[References](#)[Tables](#)[Figures](#)[⏪](#)[⏩](#)[◀](#)[▶](#)[Back](#)[Close](#)[Full Screen / Esc](#)[Printer-friendly Version](#)[Interactive Discussion](#)

fourth (FI01) is still important with 31%. In addition it has to be noted that this analysis indicates the relative role of the different corrections in the uncertainty definition but it is not related with the absolute value of the uncertainty. For DE03 the u_* have a strong effect (88%) and this is due to the differences in the three u_* thresholds selected that are the most variable compared with the other sites. Another important aspect is that the second order effects (interactions) are very low so that the three corrections seem to be independent from each other.

The NEE annual sums obtained with the different combinations of the corrections have been used as indicators of the methodological variability to analyze the effect of the different corrections on the annual balance (Fig. 9a). In the upper three panels the ranges of annual NEE due to each single correction are shown, while in the last plot the mean annual NEE and an error bar indicating minimum and maximum values obtained for each site/year. As seen before (Figs. 7, 8), the u_* filtering has the strongest impact on the data., with generally an effect on the annual sum of about $40 \text{ gC m}^{-2} \text{ yr}^{-1}$. DE03 and IT03 are the sites with the highest u_* filtering impact on the annual NEE (about $70 \text{ gC m}^{-2} \text{ yr}^{-1}$) while for other sites like FI01 and FR01 it is very small and also of the same magnitude as the storage and spike filtering effects. Looking to the annual sums it is possible to see that the uncertainties are between 15 and $100 \text{ gC m}^{-2} \text{ yr}^{-1}$ and in general between 10 and 20% except for IL01 where it is about 30% and IT03 where the effect is strong enough to change the site from sink to source. It is also interesting to note that the uncertainties are of the same magnitude of the interannual variability in the four sites where we analyzed two years. This result stresses the importance of a standardized processing to avoid the introduction of artificial between-year and between-site variability that hampers comparative analysis.

The u_* filtering has been applied to daytime and night-time data since there is still a debate on this, with part of the scientific community that applies the u_* filtering only to night-time data (Anthoni et al., 2004; Arain and Restrepo-Coupe, 2005; Haszpra et al., 2005). Figure 9b shows the same plot as Fig. 9a, but in this case we filtered only the night-time data by u_* . It is possible to see that the uncertainty due to u_* for DE03

**Algorithms and
uncertainty
processing eddy
covariance data**

D. Papale et al.

[Title Page](#)[Abstract](#)[Introduction](#)[Conclusions](#)[References](#)[Tables](#)[Figures](#)[⏪](#)[⏩](#)[◀](#)[▶](#)[Back](#)[Close](#)[Full Screen / Esc](#)[Printer-friendly Version](#)[Interactive Discussion](#)

dramatically decreases for both years and the same happens clearly to the annual budget uncertainty with a clear change also in the annual sum. For the others sites there are no major differences, including IT03 where the u_* filtering effect is still large and also increased a little. The reduction of uncertainty in DE03 can be explained by looking at the percentage of data removed by u_* filtering (Table 2): this is the site with the highest percentage of removed daytime data (up to more than 50%) and with the highest ratio between daytime and night-time data removed (up to 0.82 for DE03 2002 with u_* 95%). DE03 is also the site where the u_* threshold is the highest and also most uncertain (Fig. 3). This could be indicative for strong advection occurring also at higher u_* -values at this site, which would result in u_* filtering being not sufficient under those conditions (Kutsch et al., 2006²). For IT03 we do not see a reduction of uncertainty if we remove only the night-time data with low u_* . This is also partially related to the distribution of the filtered data between day and night because, unlike DE03, in this site the filtered data are mainly concentrated during night-time.

Since the treatment of the NEE data can also have an effect on the partitioning into GPP and TER, we have also analysed the effect of the data treatment on these flux components (Figs. 9c, d). It seems that the absolute uncertainties introduced into the GPP by the corrections are about twice as high as for the net flux. This is expected since any error on the TER estimate from the night-time data will affect the GPP estimate in the same direction and hence be partially cancelled out when looking at NEE. Moreover, the methodological variability is higher for TER than for GPP, since day- and night-time TER estimates are affected by data treatment (night-time TER is extrapolated to the day, cf. Reichstein et al., 2005), while the GPP estimates are only during day-time (during night by definition zero). As for NEE the major uncertainty is introduced by the u_* -filtering also for the flux components. Nevertheless at most sites the range of GPP and TER values obtained by different u_* -thresholds is well below $100\text{gCm}^{-2}\text{yr}^{-1}$. Since GPP and TER are large fluxes, the relative methodological

²Kutsch, W., Kolle, O., Ziegler, W., et al.: Advection and correction at Hainich, in preparation, 2006.

**Algorithms and
uncertainty
processing eddy
covariance data**

D. Papale et al.

Title Page

Abstract

Introduction

Conclusions

References

Tables

Figures

⏪

⏩

◀

▶

Back

Close

Full Screen / Esc

Printer-friendly Version

Interactive Discussion

variability of those fluxes is below 10% in most cases.

4 Conclusions

Eddy covariance data sets intercomparisons have been hampered so far by potential differences introduced by non harmonized data processing. We consider this systematic characterization of the joint effects of storage correction, spike detection and u_* -filtering on net carbon fluxes and its components GPP and TER as an important step towards a more standardized processing and to a better quantification of the uncertainties in eddy covariance data and their processing. We showed that we can strongly reduce the margin of uncertainties through a standardized processing by avoiding inappropriate data treatment (e.g. neglect storage correction or u_* -filtering), but it is also clear that heuristic methods like the u_* -filtering contain an inherent uncertainty as found by the bootstrapping approach. Large uncertainties in the u_* -thresholds at one site (and annual sums of NEE affected by those) might also indicate general limits of an insufficiency of the heuristic u_* -filtering method and standardized data processing at those sites, but it also suggest that this methodology may serve as tool to detect this problem. For a full uncertainty analysis of net CO_2 fluxes and its components estimated by eddy covariance uncertainties introduced by non-captured advection, the gap-filling methods and the flux-partitioning have to be addressed separately. Nevertheless, from our study we conclude that, except for exceptional sites, uncertainties of annual NEE and its components GPP and TER remain below $100 \text{ gC m}^{-2} \text{ yr}^{-1}$ and consequently that any spatial or temporal signals or trends that are larger than this number (e.g. continental gradients) can be detected by the eddy covariance method deployed as a coordinated network.

Acknowledgements. This work has been funded by EC project CarboeuropelP (GOCE-CT2003-505572) of the European Community. We wish to thank FLUXNET for having largely created the conditions to build up the community of flux people and the integrated data analysis.

BGD

3, 961–992, 2006

Algorithms and uncertainty processing eddy covariance data

D. Papale et al.

Title Page

Abstract

Introduction

Conclusions

References

Tables

Figures

⏪

⏩

◀

▶

Back

Close

Full Screen / Esc

Printer-friendly Version

Interactive Discussion

References

- 5 Anthoni, P., Freibauer, A., Kolle, O., and Schulze, E.-D.: Winter wheat carbon exchange in Thuringia, Germany, *Agricultural and Forest Meteorology*, 121, 55–67, 2004.
- Arain, M. A. and Restrepo-Coupe, N.: Net ecosystem production in a temperate pine plantation in southeastern Canada, *Agric. Forest Meteorol.*, 128, 223–241, 2005.
- 10 Aubinet, M., Grelle, A., Ibrom, A., Rannik, Ü., Moncrieff, J., Foken, T., Kowalski, A., Martin, P. H., Berbigier, P., Bernhofer, C., Clement, R., Elbers, J. A., Granier, A., Grunwald, T., Morgenstern, K., Pilegaard, K., Rebmann, C., Snijders, W., Valentini, R., and Vesala, T.: Estimates of the Annual Net Carbon and Water Exchange of Forest: The EUROFLUX Methodology, *Adv. Ecol. Res.*, 30, 114–173, 2000.
- Aubinet, M., Chermanne, B., Vandenhaute, M., Longdoz, B., Yernaux, M., and Laitat, E.: Long term carbon dioxide exchange above a mixed forest in the Belgian Ardennes, *Agric. Forest Meteorol.*, 108, 293–315, 2001.
- 15 Aubinet, M., Heinesch, B., and Longdoz, B.: Estimation of the carbon sequestration by a heterogeneous forest: night flux corrections, heterogeneity of the site and inter-annual variability, *Global Change Biol.*, 8, 1053–1071, 2002.
- Aubinet, M., Clement, R., Elbers, J. A., Foken, T., Grelle, A., Ibrom, A., Moncrieff, J., Pilegaard, K., Rannik, Ü., and Rebmann, C.: Methodology for Data Acquisition, Storage and Treatment, in: *Fluxes of Carbon*, edited by: Valentini, R., Water and Energy of European Forests, Springer-Verlag, Berlin, 2003a.
- 20 Aubinet, M., Heinesch, B., and Yernaux, M.: Horizontal and Vertical CO₂ Advection In A Sloping Forest, *Boundary-Layer Meteorol.*, 108, 397–417, 2003b.
- Baldocchi, D., Falge, E., Gu, L., Olson, R., Hollinger, D., Running, S., Anthoni, P., Bernhofer, C., Davis, K., Evans, R., Fuentes, J., Goldstein, A., Katul, G., Law, B., Lee, X., Malhi, Y., Meyers, T., Munger, W., Oechel, W., Paw, K. T., Pilegaard, K., Schmid, H. P., Valentini, R., Verma, S., Vesala, T., Wilson, K. and Wofsy, S.: FLUXNET: A New Tool to Study the Temporal and Spatial Variability of Ecosystem-Scale Carbon Dioxide, Water Vapor, and Energy Flux Densities, *Bull. Am. Meteorol. Soc.*, 82, 2415–2434, 2001.
- 25 Bernhofer, C., Aubinet, M., Clement, R., Grelle, A., Grünwald, T., Ibrom, A., Jarvis, P., Rebmann, C., Schulze, E.-D., and Tenhunen, J.: Spruce Forests (Norway and Sitka Spruce, Including Douglas Fir): Carbon and Water Fluxes and Balances, Ecological and Ecophysiological Determinants, in: *Fluxes of Carbon*, edited by: Valentini, R., Water and Energy of

BGD

3, 961–992, 2006

Algorithms and uncertainty processing eddy covariance data

D. Papale et al.

Title Page

Abstract

Introduction

Conclusions

References

Tables

Figures

⏪

⏩

◀

▶

Back

Close

Full Screen / Esc

Printer-friendly Version

Interactive Discussion

European Forests, Springer-Verlag, Berlin, 2003.

Cook, B. D., Davis, K. J., Wang, W., Desai, A., Berger, B. W., Teclaw, R. M., Martin, J. G., Bolstad, P. V., Bakwin, P. S., Yi, C., and Heilman, W.: Carbon exchange and venting anomalies in an upland deciduous forest in northern Wisconsin, USA, *Agric. Forest Meteorol.*, 126, 271–295, 2004.

Efron, B. and Tibshirani, R. J.: *An Introduction to the Bootstrap*, Chapman & Hall, New York, 1993.

Falge, E., Baldocchi, D., Olson, R., Anthoni, P., Aubinet, M., Bernhofer, C., Burba, G., Ceulemans, R., Clement, R., Dolman, H., Granier, A., Gross, P., Grünwald, T., Hollinger, D., Jensen, N.-O., Katul, G., Keronen, P., Kowalski, A., Lai, C. T., Law, B. E., Meyers, T., Moncrieff, J., Moors, E., Munger, J. W., Pilegaard, K., Rannik, Ü., Rebmann, C., Suyker, A., Tenhunen, J., Tu, K., Verma, S., Vesala, T., Wilson, K., and Wofsy, S.: Gap filling strategies for defensible annual sums of net ecosystem exchange, *Agric. Forest Meteorol.*, 107, 43–69, 2001.

Feigenwinter, C., Bernhofer, C., and Vogt, R.: The Influence of Advection on the Short Term CO₂ – Budget in and Above a Forest Canopy, *Boundary-Layer Meteorol.*, 113, 201–224, 2004.

Finnigan, J., Aubinet, M., Katul, G., Leuning, R., and Schimel, D.: Report of a Specialist Workshop on “Flux Measurements in Difficult Conditions”, 26–28 January, Boulder Colorado, *Bull. Am. Meteorol. Soc.*, in press, 2006.

Göckede, M., Rebmann, C., and Foken, T.: A combination of quality assessment tools for eddy covariance measurements with footprint modelling for the characterisation of complex sites, *Agric. Forest Meteorol.*, 127, 175–188, 2004.

Goulden, M. L., Munger, J. W., Fan, S. M., Daube, B. C., and Wofsy, S.: Measurements of carbon sequestration by long-term eddy covariance: methods and a critical evaluation of accuracy, *Global Change Biol.*, 2, 169–182, 1996.

Granier, A., Ceschia, E., Damesin, C., Dufrêne, E., Epron, D., Gross, P., Lebaube, S., Le Dantec, V., Le Goff, N., Lemoine, D., Lucot, E., Ottorini, J. M., Pontailier, J. Y., and Saugier, B.: The carbon balance of a young Beech forest, *Funct. Ecol.*, 14, 312–325, 2000.

Grunzweig, J. M., Lin, T., Rotenberg, E., Schwartz, A., and Yakir, D.: Carbon sequestration in arid-land forest, *Global Change Biol.*, 9, 791–799, 2003.

Gu, L., Falge, E. M., Boden, T., Baldocchi, D. D., Black, T. A., Saleska, S. R., Suni, T., Verma, S. B., Vesala, T., Wofsy, S. C., and Xu, L.: Objective threshold determination for nighttime

BGD

3, 961–992, 2006

**Algorithms and
uncertainty
processing eddy
covariance data**

D. Papale et al.

Title Page

Abstract

Introduction

Conclusions

References

Tables

Figures

◀

▶

◀

▶

Back

Close

Full Screen / Esc

Printer-friendly Version

Interactive Discussion

- eddy flux filtering, *Agric. Forest Meteorol.*, 128, 179–197, 2005.
- Haszpra, L., Barcza, Z., Davis, K. J., and Tarczay, K.: Long-term tall tower carbon dioxide flux monitoring over an area of mixed vegetation, *Agric. Forest Meteorol.*, 132, 58–77, 2005.
- Hollinger, D. and Richardson, A. D.: Uncertainty in eddy covariance measurements and its application to physiological models, *Tree Physiology*, 25, 873–885, 2005.
- 5 Knohl, A., Schulze, E.-D., Kolle, O., and Buchmann, N.: Large carbon uptake by an unmanaged 250-year-old deciduous forest in Central Germany, *Agric. Forest Meteorol.*, 118, 151–167, 2003.
- Marcolla, B., Cescatti, A., Montagnani, L., Manca, G., Kerschbaumer, G., and Minerbi, S.: Importance of advection in the atmospheric CO₂ exchanges of an alpine forest, *Agric. Forest Meteorol.*, 130, 193–206, 2005.
- 10 Massman, W. J. and Lee, X.: Eddy covariance flux corrections and uncertainties in long-term studies of carbon and energy exchanges, *Agric. Forest Meteorol.*, 113, 121–144, 2002.
- Moncrieff, J., Mahli, Y., and Leuning, R.: The propagation of errors in long-term measurements of land-atmosphere fluxes of carbon and water, *Global Change Biol.*, 2, 231–240, 1996.
- 15 Papale, D. and Valentini, R.: A new assessment of European forests carbon exchanges by eddy fluxes and artificial neural network spatialization, *Global Change Biol.*, 9, 525–535, 2003.
- Papale, D. and Reichstein, M.: Centralized quality checks and gap filling used in the CarboeuropelP Database, AmeriFlux annual meeting 2005, Boulder Colorado USA, 18–20 October 2005.
- 20 Rambal, S., Joffre, R., Ourcival, J. M., Cavender-Bares, J., and Rocheteau, A.: The growth respiration component in eddy CO₂ flux from a *Quercus ilex* mediterranean forest, *Global Change Biol.*, 10, 1460–1469, 2004.
- Reichstein, M., Tenhunen, J., Rouspard, O., Ourcival, J.-M., Rambal, S., Miglietta, F., Peressotti, A., Pecchiari, M., Tirone, G., and Valentini, R.: Inverse modeling of seasonal drought effects on canopy CO₂/H₂O exchange in three Mediterranean ecosystems, *J. Geophys. Res.*, 108, ACL 6–1 : ACL 6–16, 2003.
- 25 Reichstein, M., Falge, E., Baldocchi, D., Papale, D., Aubinet, M., Berbigier, P., Bernhofer, C., Buchmann, N., Gilmanov, T., Granier, A., Grünwald, T., Havránková, K., Ilvesniemi, H., Janous, D., Knohl, A., Laurila, T., Lohila, A., Loustau, D., Matteucci, G., Meyers, T., Miglietta, F., Ourcival, J.-M., Pumpanen, J., Rambal, S., Rotenberg, E., Sanz, M., Tenhunen, J., Seufert, G., Vaccari, F., Vesala, T., Yakir, D., and Valentini, R.: On the separation of net ecosystem exchange into assimilation and ecosystem respiration: review and improved
- 30

BGD

3, 961–992, 2006

**Algorithms and
uncertainty
processing eddy
covariance data**

D. Papale et al.

Title Page

Abstract

Introduction

Conclusions

References

Tables

Figures

◀

▶

◀

▶

Back

Close

Full Screen / Esc

Printer-friendly Version

Interactive Discussion

- algorithm, *Global Change Biol.*, 11, 1424–1439, 2005.
- Richardson, A. D., Hollinger, D. Y., Burba, G. G., Davis, K. J., Flanagan, L. B., Katul, G. G., William Munger, J., Ricciuto, D. M., Stoy, P. C., Suyker, A. E., Verma, S. B., and Wofsy, S. C.: A multi-site analysis of random error in tower-based measurements of carbon and energy fluxes, *Agric. Forest Meteorol.*, 136, 1–18, 2006.
- 5 Sachs, L.: *Angewandte Statistik: Anwendung Statistischer Methoden*, Springer, Berlin, 1996.
- Staebler, R. M. and Fitzjarrald, D. R.: Observing subcanopy CO₂ advection, *Agric. Forest Meteorol.*, 122, 139–156, 2004.
- 10 Suni, T., Rinne, J., Reissell, A., Altimir, N., Keronen, P., Rannik, Ü., Dal Maso, M., Kulmala, M., and Vesala, T.: Long-term measurements of surface fluxes above a Scots pine forest in Hyttiala, southern Finland, 1996–2001, *Boreal Environ. Res.*, 8, 287–301, 2003.
- Tedeschi, V., Rey, A. N. A., Manca, G., Valentini, R., Jarvis, P. G., and Borghetti, M.: Soil respiration in a Mediterranean oak forest at different developmental stages after coppicing, *Global Change Biol.*, 12, 110–121, 2006.
- 15 Wohlfahrt, G., Anfang, C., Bahn, M., Haslwanger, A., Newesely, C., Schmitt, M., Drösler, M., Pfadenhauer, J., and Cernusca, A.: Quantifying nighttime ecosystem respiration of a meadow using eddy covariance, chambers and modelling, *Agric. Forest Meteorol.*, 128, 141–162, 2005.

BGD

3, 961–992, 2006

**Algorithms and
uncertainty
processing eddy
covariance data**

D. Papale et al.

Title Page

Abstract

Introduction

Conclusions

References

Tables

Figures

⏪

⏩

◀

▶

Back

Close

Full Screen / Esc

Printer-friendly Version

Interactive Discussion

Table 1. Sites and years used and main characteristics. MF=mixed forest, ENF=evergreen needle forest, EBF=evergreen broadleaves forest, DBF=deciduous broadleaves forest, ECO=Ecosystem type, MAT=Mean Annual Temperature (°C), Prec=Annual precipitation (mm).

Code	Years	Name	Lat.	Long.	ECO	MAT	Prec	Reference
BE01	2001	Vielsalm	50°18' N	5°59' E	MF	7.5	1000	Aubinet et al. (2001)
DE02	2001, 2002	Tharandt	50°57' N	13°34' E	ENF	7.7	820	Bernhofer et al. (2003)
DE03	2001, 2002	Hainich	51°04' N	10°27' E	DBF	6.8	775	Knohl et al. (2003)
FI01	2001, 2002	Hyytiälä	61°50' N	24°17' E	ENF	3.8	709	Suni et al. (2003)
FR01	2001, 2002	Hesse	48°40' N	07°03' E	DBF	9.9	975	Granier et al. (2000)
FR04	2002	Puechabon	43°44' N	03°35' E	EBF	13.5	872	Rambal et al. (2004)
IL01	2002	Yatir	31°20' N	35°03' E	ENF	18.2	280	Grunzweig et al. (2003)
IT03	2002	Roccarespampani	42°24' N	11°55' E	DBF	15.2	876	Tedeschi et al. (2006)

Title Page

Abstract

Introduction

Conclusions

References

Tables

Figures

⏪

⏩

◀

▶

Back

Close

Full Screen / Esc

Printer-friendly Version

Interactive Discussion

Algorithms and uncertainty processing eddy covariance data

D. Papale et al.

Table 2. Percentage of half hourly data (storage corrected with the best method available at each site: BE01, DE02, DE03 and FI01 profile, FR01, FR04, IL01 and IT03 discrete approach) deleted in the different conditions. Missing: data not measured or deleted due to evident technical problems, Spike: additional data removed with the spike detection technique according with the different thresholds, u_* : additional data removed (after previous removal of spikes using threshold 5.5) due to low u_* conditions according with the three different thresholds, Total: the percentage of data removed summing missing data, spike with $z=5.5$ and u_* 50%. The two numbers in italic are the percentages of night-time and daytime respectively for each site. All the percentages are relative to the year.

Site_year	Missing	Spike 4	Spike 5.5	Spike 7	Ustar 5%	Ustar 50%	Ustar 95%	Total
BE01_01	7.48	<i>7.03</i>	<i>1.11</i>	<i>0.38</i>	<i>0.13</i>	<i>20.03</i>	<i>29.82</i>	<i>37.23</i>
		7.92	1.06	1.02	0.46	0.54	0.19	0.26
DE02_01	9.82	<i>8.61</i>	<i>2.28</i>	<i>1.36</i>	<i>0.68</i>	<i>13.35</i>	<i>17.45</i>	<i>28.15</i>
		11.04	1.89	1.50	0.67	0.23	4.83	6.76
DE02_02	16.64	<i>14.21</i>	<i>2.31</i>	<i>1.40</i>	<i>0.64</i>	<i>18.74</i>	<i>24.52</i>	<i>40.14</i>
		19.08	1.76	1.21	0.95	0.49	0.41	0.18
DE03_01	15.55	<i>17.80</i>	<i>1.44</i>	<i>0.64</i>	<i>0.30</i>	<i>25.83</i>	<i>38.93</i>	<i>57.36</i>
		13.30	1.30	1.16	0.58	0.53	0.24	0.18
DE03_02	15.67	<i>18.58</i>	<i>1.05</i>	<i>0.62</i>	<i>0.29</i>	<i>35.42</i>	<i>47.35</i>	<i>66.55</i>
		12.76	1.20	1.35	0.64	0.66	0.30	0.32
FI01_01	14.25	<i>19.38</i>	<i>1.58</i>	<i>0.76</i>	<i>0.38</i>	<i>21.15</i>	<i>28.92</i>	<i>49.06</i>
		9.12	1.27	0.97	0.59	0.41	0.29	0.21
FI01_02	15.59	<i>21.76</i>	<i>1.40</i>	<i>0.62</i>	<i>0.23</i>	<i>28.53</i>	<i>37.63</i>	<i>60.00</i>
		9.42	1.27	1.13	0.51	0.41	0.19	0.15
FR01_01	7.63	<i>8.94</i>	<i>3.08</i>	<i>2.04</i>	<i>1.12</i>	<i>23.29</i>	<i>23.29</i>	<i>26.75</i>
		6.31	2.84	2.60	1.87	1.70	1.13	1.14
FR01_02	8.41	<i>9.24</i>	<i>3.46</i>	<i>1.91</i>	<i>1.04</i>	<i>24.08</i>	<i>24.19</i>	<i>28.55</i>
		7.58	2.63	1.80	1.60	1.29	0.87	0.70
FR04_02	9.51	<i>9.92</i>	<i>2.18</i>	<i>1.00</i>	<i>0.43</i>	<i>46.77</i>	<i>52.67</i>	<i>63.60</i>
		9.10	1.88	1.59	0.86	0.71	0.41	0.38
IL01_02	18.20	<i>17.32</i>	<i>1.87</i>	<i>1.12</i>	<i>0.63</i>	<i>38.66</i>	<i>46.70</i>	<i>55.37</i>
		19.09	1.67	1.47	0.92	0.72	0.48	0.33
IT03_02	6.96	<i>6.54</i>	<i>2.71</i>	<i>1.82</i>	<i>0.96</i>	<i>34.20</i>	<i>45.37</i>	<i>53.72</i>
		7.39	2.40	2.09	1.61	1.40	0.86	0.75

Title Page

Abstract Introduction

Conclusions References

Tables Figures

◀ ▶

◀ ▶

Back Close

Full Screen / Esc

Printer-friendly Version

Interactive Discussion

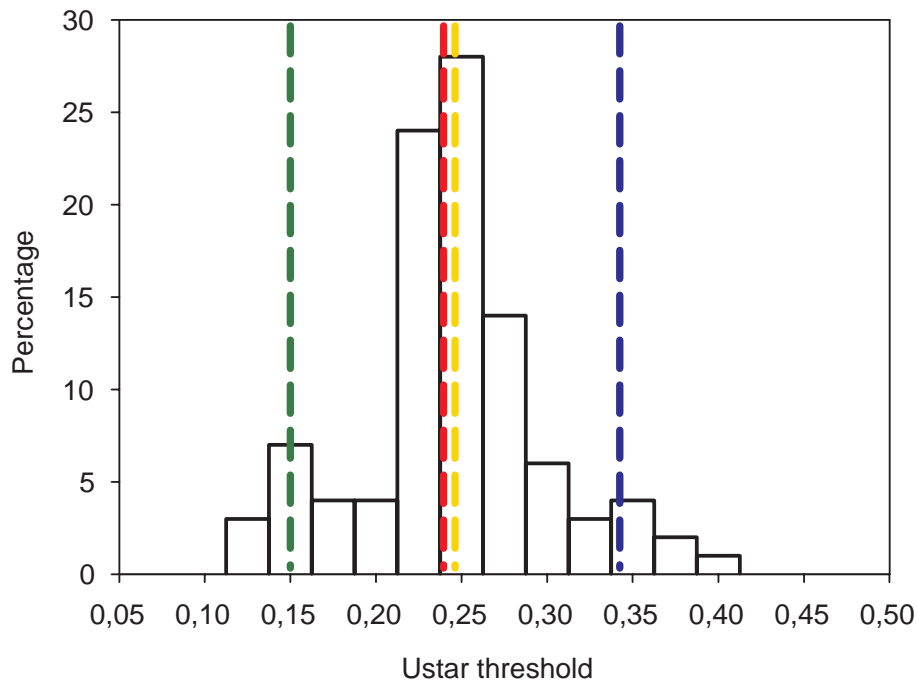


Fig. 1. Example of the different u_* threshold found with the bootstrapping. Lines indicate mean (yellow), median (red), 5% (green) and 95% (blue) values. BE01_01, storage with discrete approach, spikes threshold $z=5.5$.

Title Page

Abstract

Introduction

Conclusions

References

Tables

Figures

⏪

⏩

◀

▶

Back

Close

Full Screen / Esc

Printer-friendly Version

Interactive Discussion

Algorithms and uncertainty processing eddy covariance data

D. Papale et al.

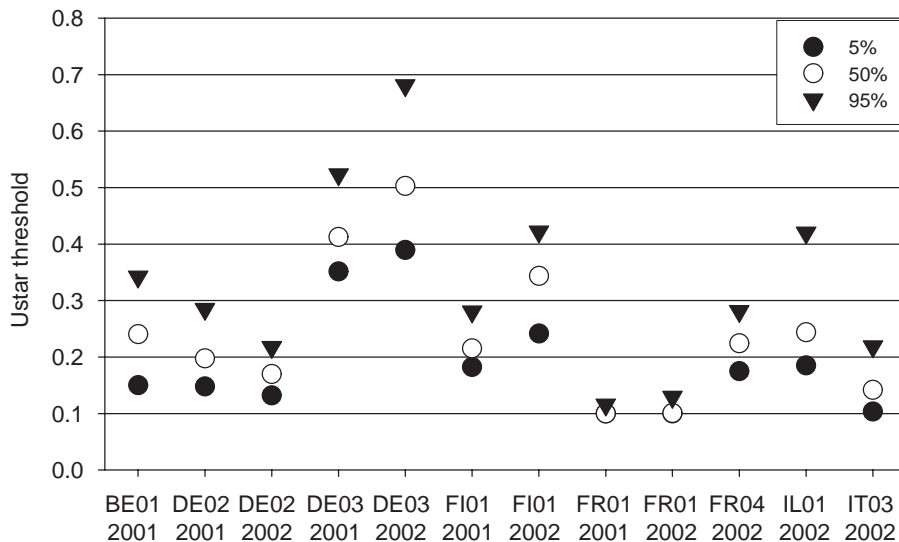


Fig. 2. Different u_* threshold values selected for the 12 yearly datasets for discrete approach storage calculation and spike threshold $z=5.5$.

Title Page

Abstract

Introduction

Conclusions

References

Tables

Figures

⏪

⏩

◀

▶

Back

Close

Full Screen / Esc

Printer-friendly Version

Interactive Discussion

Algorithms and uncertainty processing eddy covariance data

D. Papale et al.

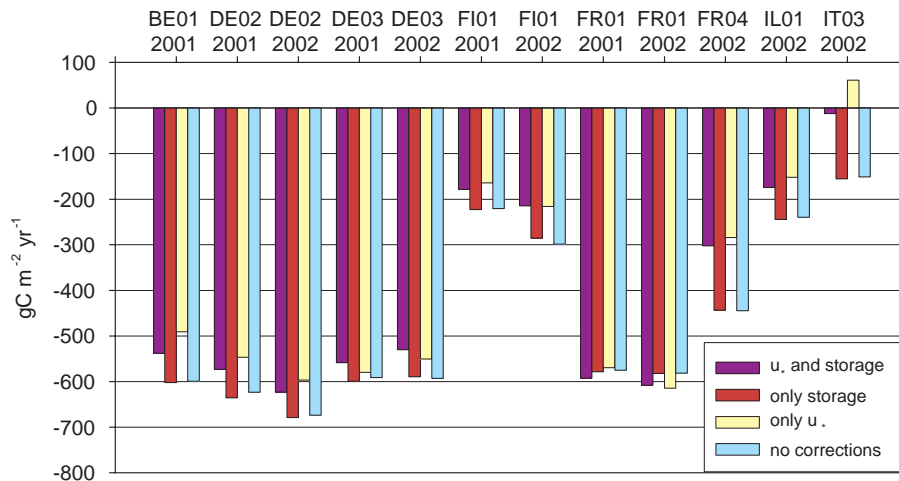


Fig. 3. Effect of storage and u* corrections on annual sums.

Title Page	
Abstract	Introduction
Conclusions	References
Tables	Figures
◀	▶
◀	▶
Back	Close
Full Screen / Esc	
Printer-friendly Version	
Interactive Discussion	

Algorithms and uncertainty processing eddy covariance data

D. Papale et al.

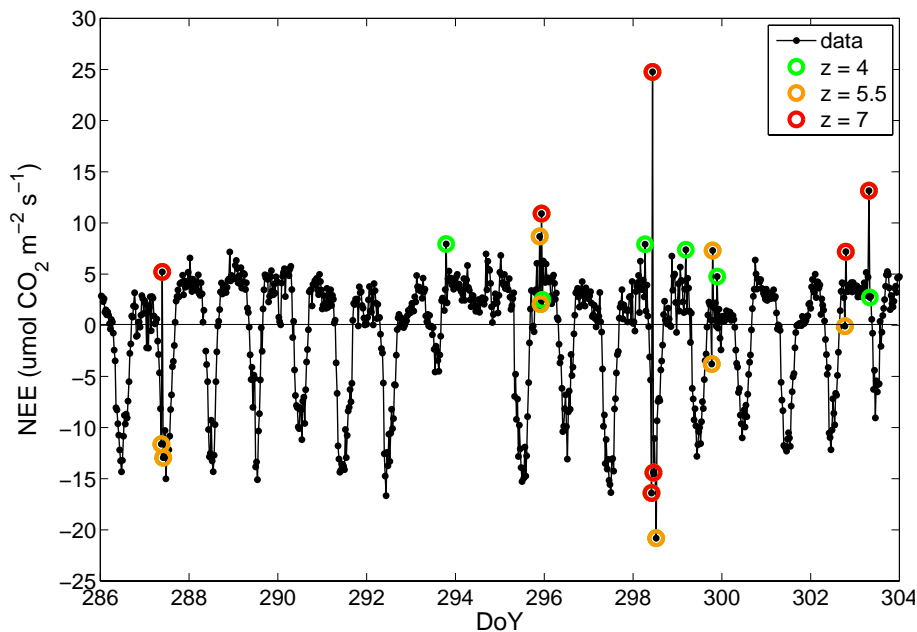


Fig. 4. Examples of NEE half hourly data detected as spikes using the different thresholds (z values). Site: FR04.02.

Title Page

Abstract

Introduction

Conclusions

References

Tables

Figures

◀

▶

◀

▶

Back

Close

Full Screen / Esc

Printer-friendly Version

Interactive Discussion

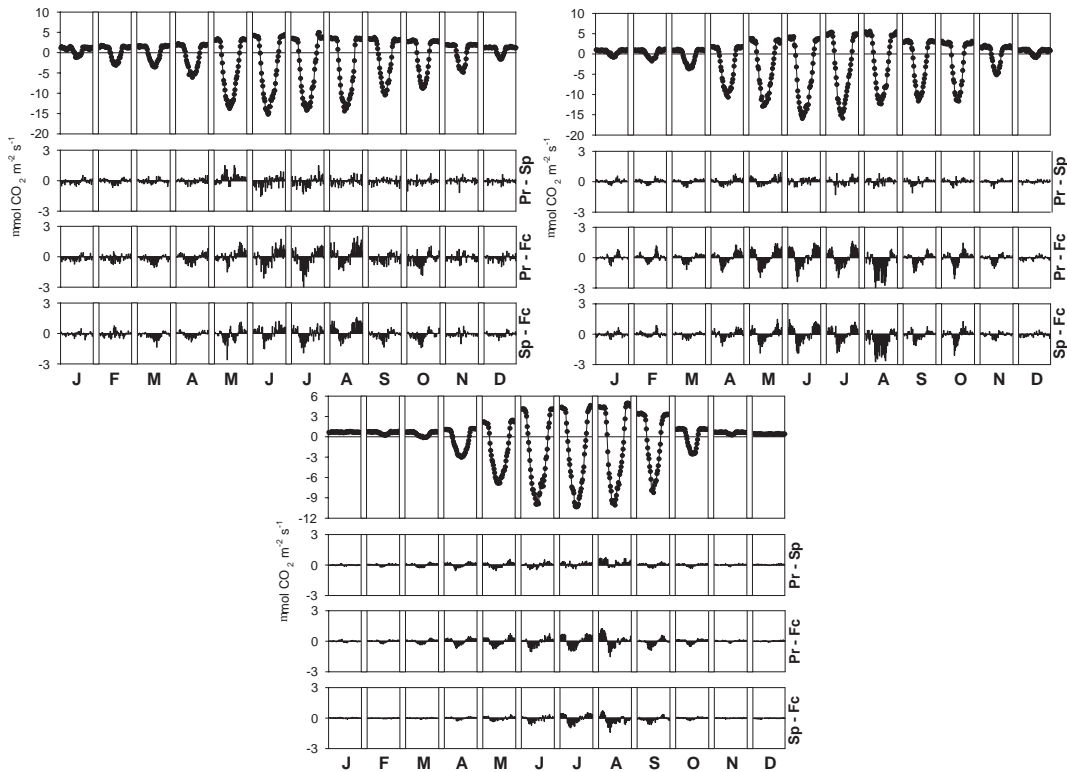


Fig. 5. Effect of different storage measurement methods on monthly mean diurnal NEE trends for three sites: BE01.01 (Fig. 5a), DE02.01 (Fig. 5b) and FI01.02 (Fig. 5c). In the upper panel diurnal trend calculated from NEE_{pr} is shown; the others three panels the residuals respectively between the two storages (Pr–Sp), between storage from profile and no storage correction (Pr–Fc) and between storage from discrete approach and no storage correction (Sp–Fc).

Title Page

Abstract

Introduction

Conclusions

References

Tables

Figures

◀

▶

◀

▶

Back

Close

Full Screen / Esc

Printer-friendly Version

Interactive Discussion

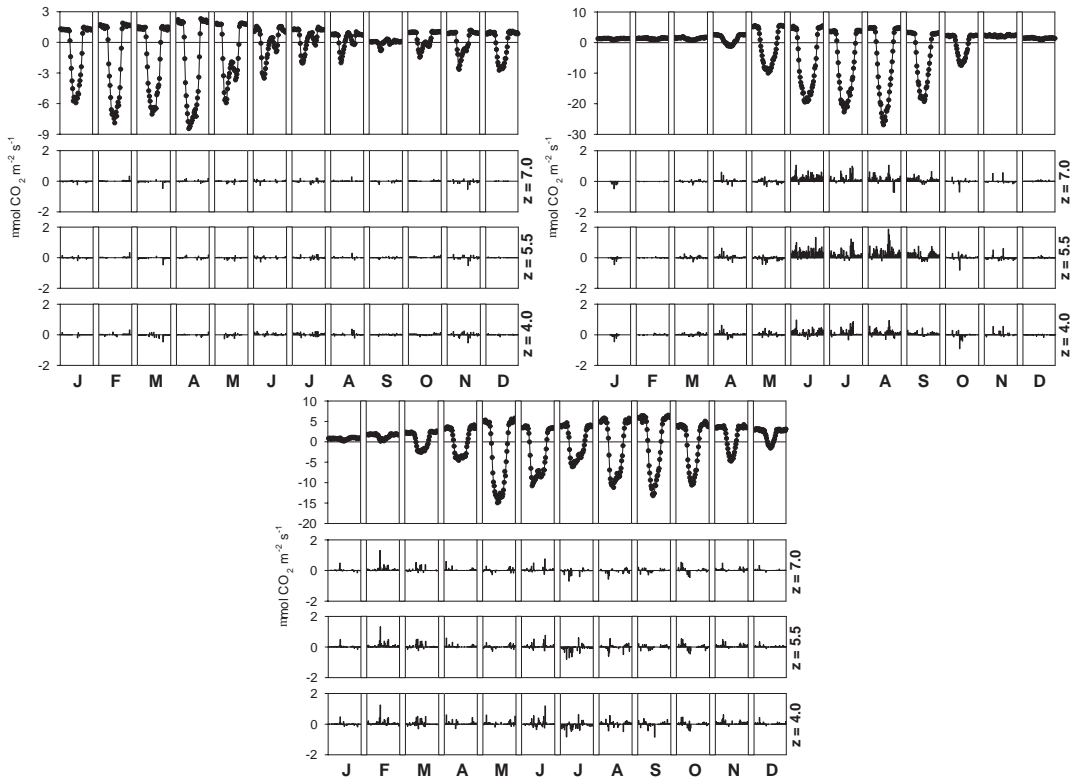


Fig. 6. Effect of different spike detection thresholds z on monthly mean diurnal NEE trends for three sites: IL01_02 (Fig. 6a), DE03_02 (Fig. 6b) and IT03_02 (Fig. 6c). In the upper panel diurnal trend calculated from data before spike detection is shown; the others three panels the residuals respectively between original and $z=7$, between original and $z=5.5$ and between original and $z=4$.

Title Page

Abstract

Introduction

Conclusions

References

Tables

Figures

◀

▶

◀

▶

Back

Close

Full Screen / Esc

Printer-friendly Version

Interactive Discussion

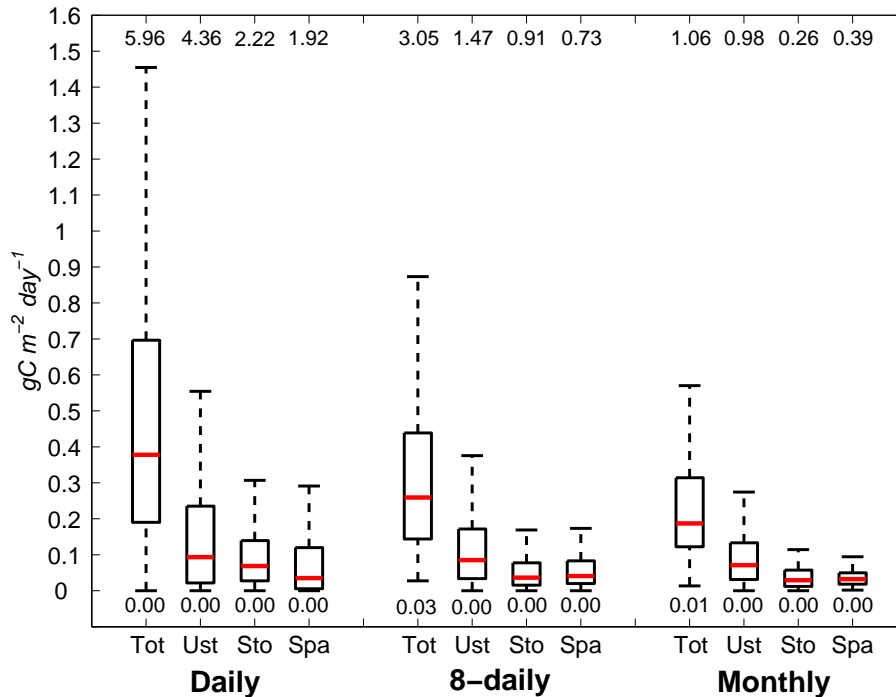


Fig. 7. Contribution of the different corrections (storage, u_* , spike) and total effect on daily, 8-daily and monthly sums. Boxplots indicate the range of values obtained applying respectively all the corrections (Tot), the three different u_* thresholds with the best storage possible and spike 5.5 (Ust), the two different storage calculation methods with u_* 50% and spike 5.5 (Sto) and the three different z -values for the spike detection with the best storage possible and u_* 50% (Spa). The red line indicates the median, the box the 50% percentiles and the black lines extending above and below the box show the extent of the rest of the sample (unless there are outliers). In this plot an outlier is a value that is more than 1.5 times the interquartile range away from the top or bottom of the box. The minimum and maximum outliers values are however reported above the plot.

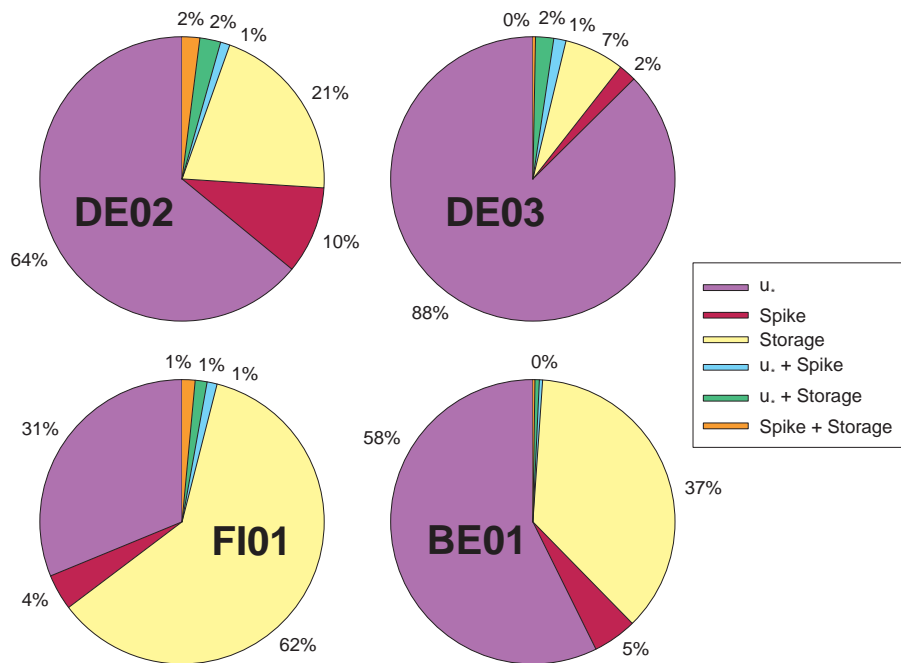


Fig. 8. Results of the ANOVA test on the four sites where both the methods to measure the storage flux have been available.

Title Page	
Abstract	Introduction
Conclusions	References
Tables	Figures
⏪	⏩
◀	▶
Back	Close
Full Screen / Esc	
Printer-friendly Version	
Interactive Discussion	

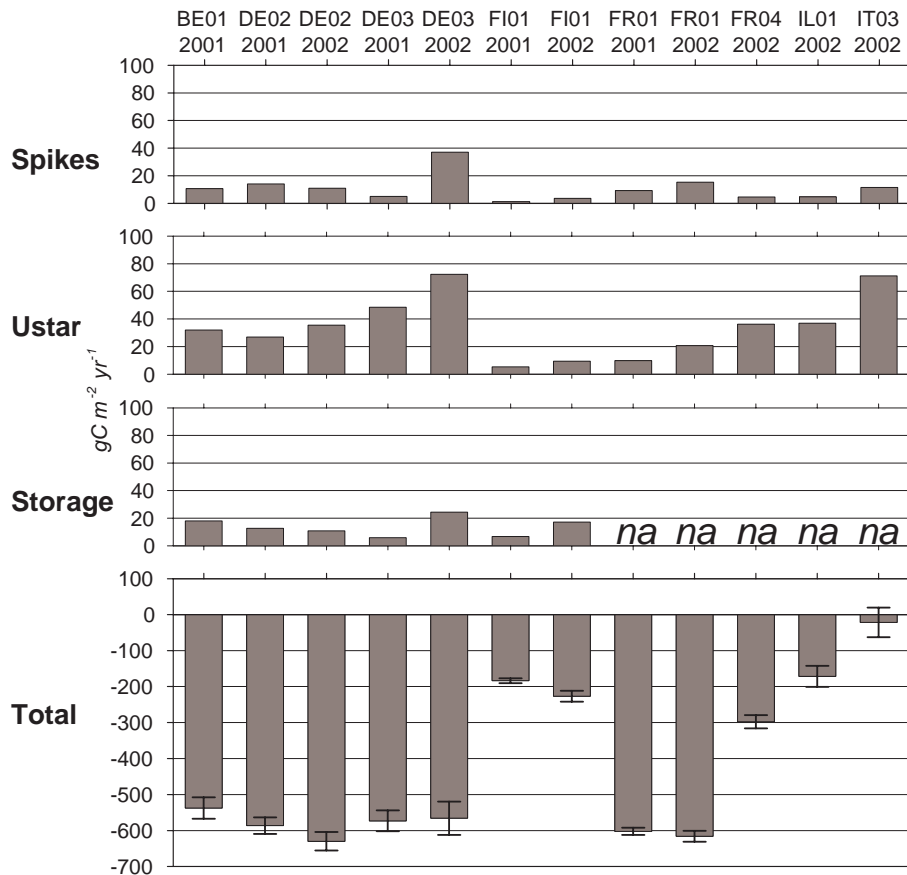


Fig. 9a. Effect of the three different corrections and total uncertainty introduced on the annual NEE for the different sites and years. u_* correction applied to daytime and night-time data. Ranges calculated taking into account 4 spikes detection level (0, 4, 5.5, 7), 3 u_* thresholds (5%, 50%, 95%) and 2 storages calculation (single point and profile when available, na = not available).

Title Page

Abstract

Introduction

Conclusions

References

Tables

Figures

◀

▶

◀

▶

Back

Close

Full Screen / Esc

Printer-friendly Version

Interactive Discussion

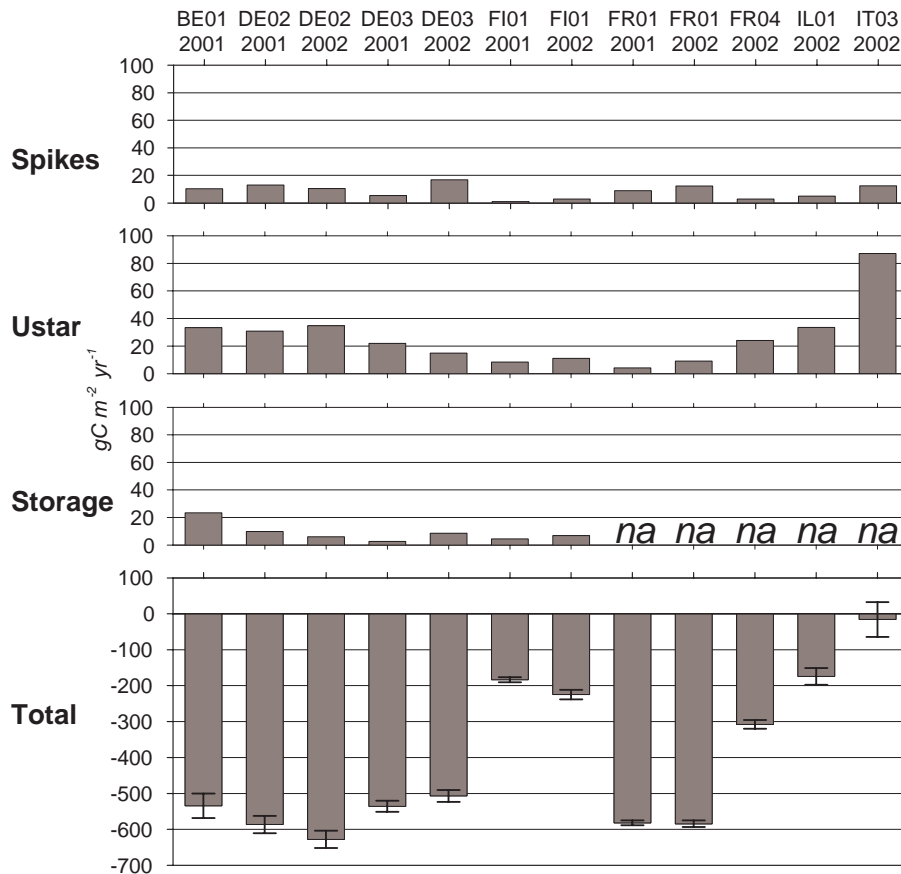


Fig. 9b. Effect of the three different corrections and total uncertainty introduced on the annual NEE for the different sites and years. u_* correction applied only to night-time data. Ranges calculated taking into account 4 spikes detection level (0, 4, 5.5, 7), 3 u_* thresholds (5%, 50%, 95%) and 2 storages calculation (single point and profile when available).

Title Page	
Abstract	Introduction
Conclusions	References
Tables	Figures
◀	▶
◀	▶
Back	Close
Full Screen / Esc	
Printer-friendly Version	
Interactive Discussion	

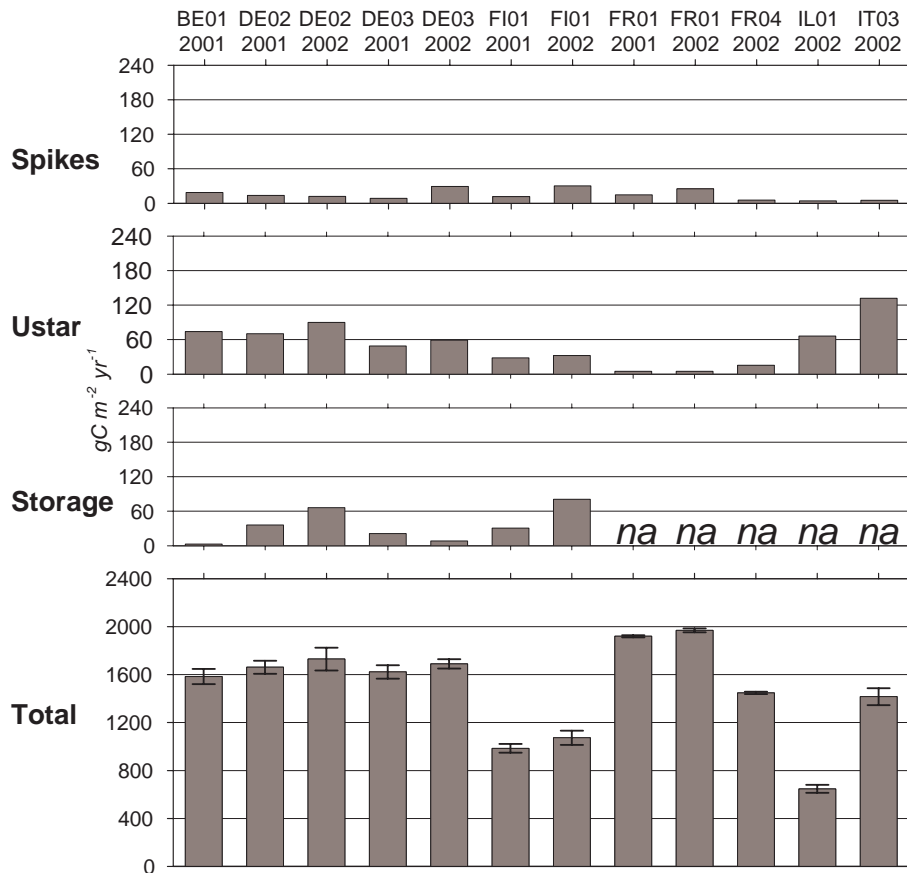


Fig. 9c. Effect of the three different corrections and total uncertainty introduced on the annual GPP for the different sites and years. u_* correction applied to daytime and night-time data. Ranges calculated taking into account 4 spikes detection level (0, 4, 5.5, 7), 3 u_* thresholds (5%, 50%, 95%) and 2 storages calculation (single point and profile when available).

Title Page

Abstract Introduction

Conclusions References

Tables Figures

⏪ ⏩

◀ ▶

Back Close

Full Screen / Esc

Printer-friendly Version

Interactive Discussion

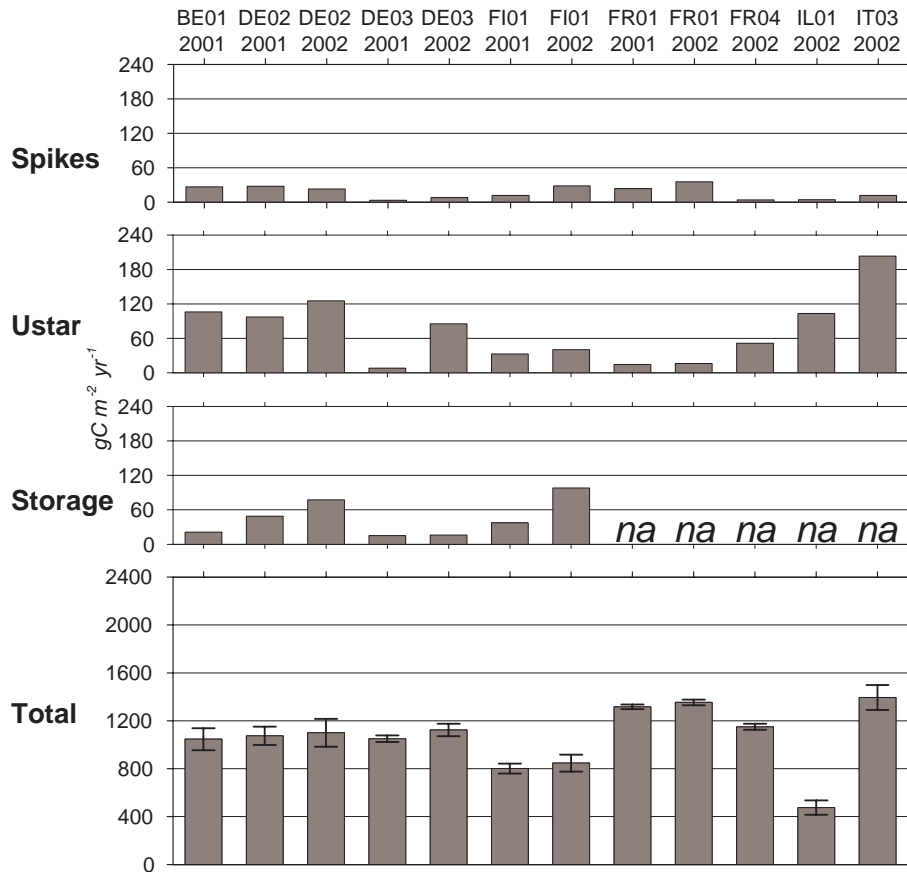


Fig. 9d. Effect of the three different corrections and total uncertainty introduced on the annual TER for the different sites and years. u_s correction applied to daytime and night-time data. Ranges calculated taking into account 4 spikes detection level (0, 4, 5.5, 7), 3 u_s thresholds (5%, 50%, 95%) and 2 storages calculation (single point and profile when available).